Observational evidence of coupling between quasi-periodic echoes and medium scale traveling ionospheric disturbances

S. Saito, M. Yamamoto, H. Hashiguchi, A. Maegawa, A. Saito

**Annales
Geophysicae**

Observational evidence of coupling between quasi-periodic echoes and medium scale traveling ionospheric disturbances

S. Saito[1], M. Yamamoto[2], H. Hashiguchi[2], A. Maegawa[2], and A. Saito[3]

[1]National Institute of Information and Communications Technology, Nukui-kita 4-2-1, Koganei, Tokyo 184-8795, Japan
[2]Research Institute for Sustainable Humanosphere, Kyoto University, Gokasho, Uji, Kyoto 611-0011, Japan
[3]Department of Geophysics, Faculty of Science, Kyoto University, Japan

Abstract. We have found that quasi-periodic (QP) echoes in the E region were well defined when medium scale traveling ionospheric disturbances (MSTIDs) in the F region were present. The appearance and disappearance of the MSTIDs observed with the dense GPS receiver network are well correlated with the development and decay of QP echoes observed with the Middle-and-Upper atmosphere (MU) radar. Interferometric imaging of the QP echoes obtained using the MU radar shows that bands of echoing regions aligned northwest to southeast drift southwestward, and their wavefront and propagation direction are the same as those of MSTIDs. This result confirms the expectation of Hysell et al. (2002) who observed band structures in QP echoes by using the MU radar and suggested their relation to MSTIDs. We found observational evidence that the midlatitude E- and F regions are coupled through the geomagnetic field line, although we could not clearly ascertain which of the two regions is the source.

Keywords. Ionosphere (Ionospheric irregularities; Mid-latitude ionosphere; Plasma waves and instabilities)

1 Introduction

Medium-scale traveling ionospheric disturbances (MSTIDs) are one kind of ionospheric disturbances observed in the mid-latitude F region. Two-dimensional structures of night-time MSTIDs have been studied with optical (Mendillo et al. , 1997; Garcia et al., 2000; Kubota et al., 2000) or radio techniques (Saito et al., 1998). They propagate southwestward with typical wavelengths of 100–500 km. This preferred propagation direction is often explained by an electrodynamic plasma instability proposed by Perkins (1973), the Perkins instability. However, as is known, the growth

Correspondence to: S. Saito
(susaito@nict.go.jp)

rate of the Perkins instability is too small to explain the phenomenon.

The quasi-periodic (QP) echoes associated with the sporadic E (E_s) layer are known to often propagate southwestward (Yamamoto et al., 1997; Tsunoda et al., 2004), in the same preferred propagation direction as MSTIDs. Cosgrove and Tsunoda (2004) have shown that electric coupling between the midlatitude E- and F regions accelerates plasma instabilities both in the E- and F regions (see also Tsunoda and Cosgrove, 2001). They have pointed out that the growth rate of the E-F coupled-layer instability is greater than that of the Perkins instability loaded by a static E_s layer and that of E_s layer instability loaded by a static F layer (Cosgrove and Tsunoda, 2002). Some case studies indicate that the E- and F regions are coupled to each other in the midlatitude ionosphere (Haldoupis et al., 2003; Kelley et al., 2003). Recently, Yamamoto et al. (private communication) found that VHF radar backscatter from field-aligned plasma irregularities (FAIs) exist simultaneously in the E- and F regions on the same magnetic field lines, indicating existence of close coupling between the E- and F regions. Hysell et al. (2002) found that "ribbon" structures that are aligned northwest to southeast and propagate southwestward are sometimes observed in the QP echoes. They hypothesized that the ribbon structure might be related to MSTIDs. However, they had no information on activities of MSTIDs.

The GEONET is the dense GPS receiver network installed and operated by the Geographical Survey Institute of Japan; the network consists of more than 1000 GPS receivers all over Japan. By using GEONET, Saito et al. (1998) found that two-dimensional total electron contents (TECs) maps were very effective for detecting TIDs (see also Saito et al., 2002) in the F region. The TEC observation enables the monitoring of MSTIDs regardless of weather.

Kyoto University has been operating the MU radar at Shigaraki, Japan. The MU radar has been used to detect backscatter from plasma irregularities in both the E region
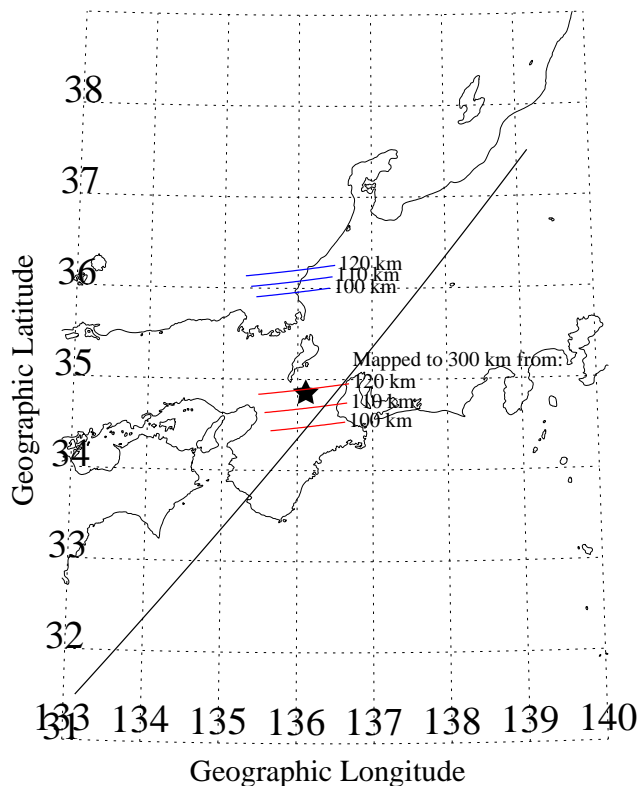
Fig. 1. Geometry of observed regions. Loci of perpendicularity at 100, 110, and 120 km for the MU radar are indicated by blue lines. At the beam center, the ranges from the MU radar corresponding to 100, 110, and 120 km are 159.5, 176.3, and 193.2 km, respectively. Red lines indicate the loci of perpendicularity mapped up to 300 km along the geomagnetic field line.

(e.g., Yamamoto et al., 1991) and the F region (e.g., Fukao et al., 1991). The combination of the GEONET and the MU radar observations is very unique and effective for studying MSTIDs and their relationship to the E region.

In this study, we report how we examined the coupling processes between the mid-latitude E- and F regions by observing QP echoes with the MU radar and simultaneously observing MSTIDs by using GEONET.

2 Observations

2.1 QP echoes

We observed QP echoes with the MU radar at Shigaraki (34.9° N, 136.1° E), Japan on four nights from 30 May to 2 June 2005. The operation frequency was 46.5 MHz, and the peak power was 1 MW. We adopted a 16-bit complementary code with a sub-pulse length of $4 \, \mu s$, corresponding to the range resolution of 0.6 km. The inter-pulse period was 2.25 ms corresponding to the non-aliased Doppler velocity range of $\pm 358 \, \mathrm{m \, s^{-1}}$. The transmission beam was pointed

nearly to the geomagnetic north (Azimuth: $-4.3°$, Zenith: $50.84°$). Signals were received independently by 25 antenna groups that enabled two-dimensional interferometric imaging. We used 19 antenna groups with the same regular hexagonal shape for our analysis; these antenna groups achieve 30 non-redundant baselines. Images of radar echoes were obtained every 4.608 s at three Doppler velocity ranges -269 to $-90 \, \mathrm{m \, s^{-1}}$, -90 to $+90 \, \mathrm{m \, s^{-1}}$, and $+90$ to $+269 \, \mathrm{m \, s^{-1}}$. The positive (negative) Doppler velocity refers to motion away (toward) the radar. We used the same MU radar imaging technique as that described in Saito et al. (2006). Figure 1 shows the observation region of our study. The E-region echoes are typically observed at altitudes of 100–120 km. The MU radar is sensitive to the E region FAI 100–200 km to the north of the radar (blue lines in Fig. 1). The observation area is mapped along the geomagnetic field lines to the F region at an altitude of 300 km that is 0–100 km south of the MU radar (red lines in Fig. 1). In addition to these observations, ionograms were obtained every 15 min during the experiment with the ionosonde at the MU radar site. The data were used to show the background condition of the ionosphere.

2.2 Total Electron Contents (TECs) variation

TECs between the GEONET receivers and the GPS satellites can be derived from the relative delay between the two carrier waves with different frequencies. They were derived every 30 s. A detailed description of how TECs were estimated was given by Saito et al. (1998). TECs along the satellite-receiver path are converted to vertical values by assuming that the contributions to the slant TECs are all from a virtual thin layer at an altitude of 300 km. Data from GPS satellites with elevation angles lower than 35° were not used in this analysis. For each satellite-receiver paths available, a moving average of TECs over one hour was subtracted from the TEC data to provide a perturbation component.

3 Results

3.1 Occurrences of QP Echoes and MSTIDs

Figure 2 shows Range-Time-Intensity (RTI) maps of echo power observed using the MU radar on the four nights from 30 May to 2 June 2005. The observation period of each date was limited to nighttime. We observed intense echoes during the experiment except for the night of 30 May 2005. Among those intense echoes, well-defined QP echoes were observed 22:00–23:30 JST on 31 June 2005, 19:45–00:30 JST on 1 June 2005, and 20:30–22:15 JST on 2 June 2005. Although we observed FAI echoes after 22:15 JST on 2 June 2005, the QP striations were not clear. Figure 3 shows examples of TEC perturbation maps on the four nights previously mentioned. The time when the TEC map was obtained on each night is indicated by a square symbol in each panel of Fig. 2.
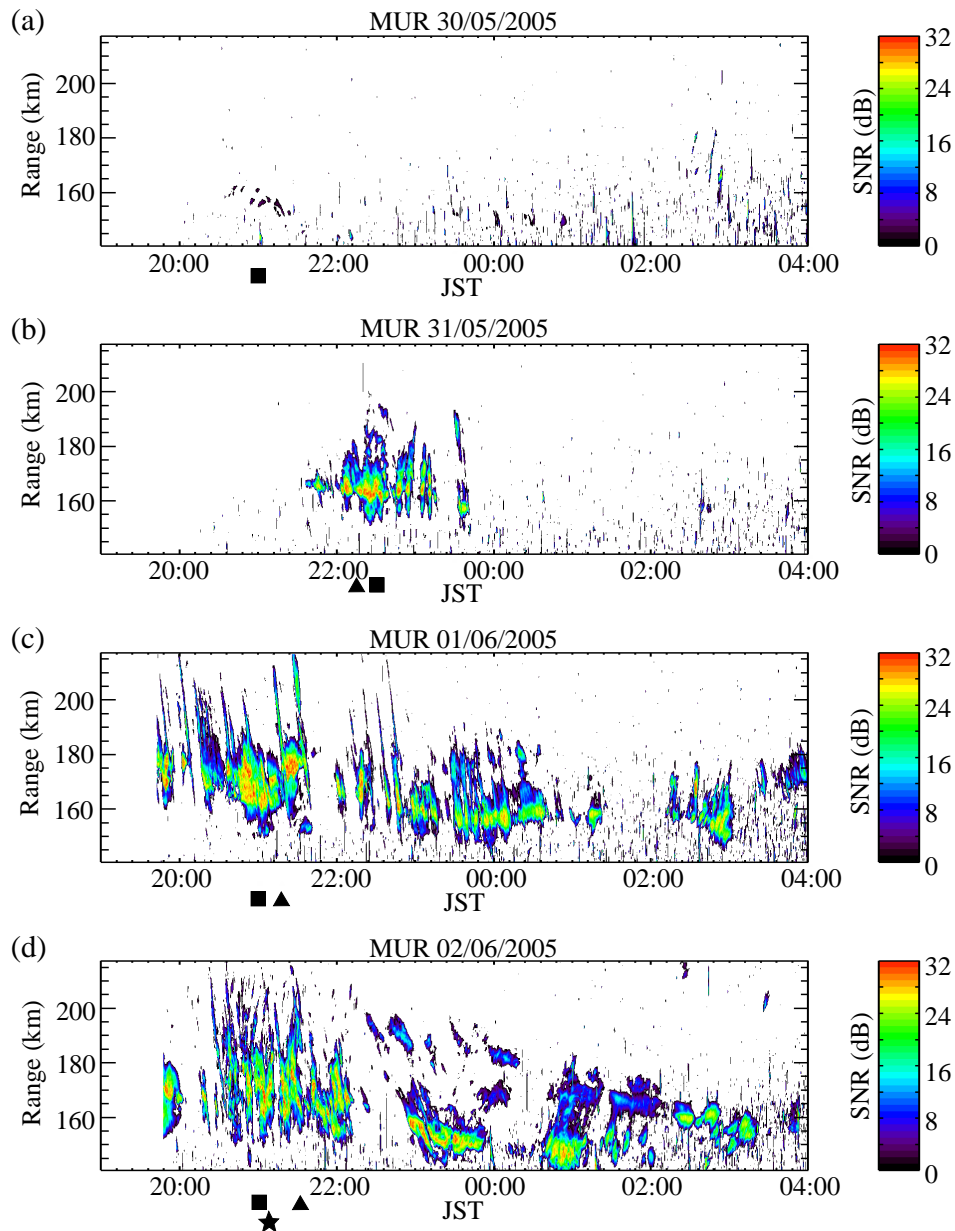
Fig. 2. Range-Time-Intensity plots of echo power observed with the MU radar. **(a–d)** correspond to four successive nights from 30 May to 2 June 2005, respectively. Squares (□), a star (⋆) and triangles (△) in the figures designate the time of events shown in Figs. 3, 5, and 6, respectively.

When the well-defined QP echoes were observed on 31 May, 1 June, and 2 June 2005, TECs showed wave-like perturbation stretched from northwest to southeast and propagating southwestward (Figs. 3b–d). In contrast, TEC distribution at a similar local time on 30 May 2005 was less structured compared to the other nights (Fig. 3a). The absolute and relative amplitudes (peak-to-peak) of TEC perturbation in Figs. 3b–d were 1.6, 0.6, and 2.8 TECU (1 TECU=10^{16} m^{-2}), and 16, 10, and 16%, respectively. A typical wavelength was about 150 km. To see the MSTID activity more clearly, time se-

ries of TEC perturbations along the line from northeast to southwest that is indicated in Fig. 1 are plotted in Fig. 4 (in the so-called keogram format). It should be noted that the latitude/longitude ranges of Fig. 4 are wider than those of Fig. 3. The analysis period is identical to that of Fig. 2. The TEC perturbations occur in the F region. We selected the area of interest that is connected to the E region observed by the MU radar. Downward-sloping stripes in the figures indicate MSTIDs propagating southwestward. MSTIDs were identified from the keograms 02:30–04:00 JST and
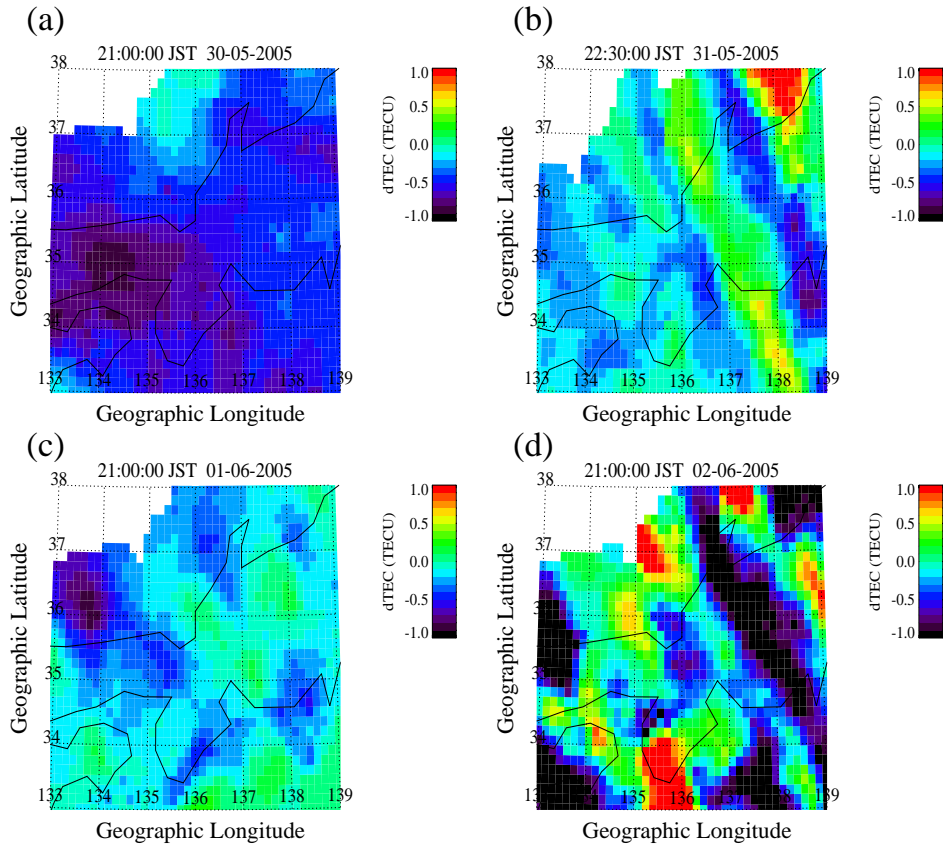
Fig. 3. Examples of TEC perturbation maps observed with GEONET. **(a–d)** were obtained at the times that are indicated by squares in Figs. 2a–d and Figs. 4a–d, respectively.

Table 1. Periods when the activities of MSTIDs and QP echoes were high.

Date	Occurrence Periods (JST)	
(start of the night)	MSTIDs	QP echoes
30 May 2005	02:30–04:00 (on 31 May 2005)	not active
31 May 2005	22:10–24:00	22:00–23:30
1 June 2005	20:30–00:30	19:45–00:30
2 June 2005	20:10–22:20	20:30–22:15

Table 2. Peak-to-peak amplitudes of TEC variations of MSTIDs and Doppler velocities of QP echoes.

Date	Peak-to-peak Amplitudes	
	MSTIDs (TECU)	QP echoes (m s^{-1})
31 May 2005	0.97	341
1 June 2005	0.96	326
2 June 2005	1.83	432

22:10–24:00 JST on 31 May 2005, 20:30–00:30 JST on 1 June 2005, and 20:10–22:20 JST on 2 June 2005. Table 1 summarizes the active periods of the MSTIDs and the QP echoes. The activity of the MSTIDs and QP echoes in field-associated F- and E regions were very well coincided except for the period 02:30–04:00 JST on 31 May 2005.

3.2 Fine structure of QP echoes and MSTIDs

During the periods when well-defined QP echoes were observed, two-dimensional radar interferometric imaging showed that many band structures of echoing regions aligned northwest to southeast drifted southwestward. Examples of such drifting bands that we observed on 2 June 2005 are shown in Fig. 5. The propagation speed of the drifting band was about 90 m s^{-1}. These structures are very similar to "ribbons" reported by Hysell et al. (2002).

At the same time we observed such bands with the MU radar, we found MSTIDs in TEC variations with wavefronts aligned northwest to southeast and propagating southwestward. The propagation speed of the MSTIDs estimated by using the slope of stripes in Fig. 4 was about 110 m s^{-1}. Two wave-like structures in the E- and F region propagated in the same direction with similar velocities. Figure 6 also shows
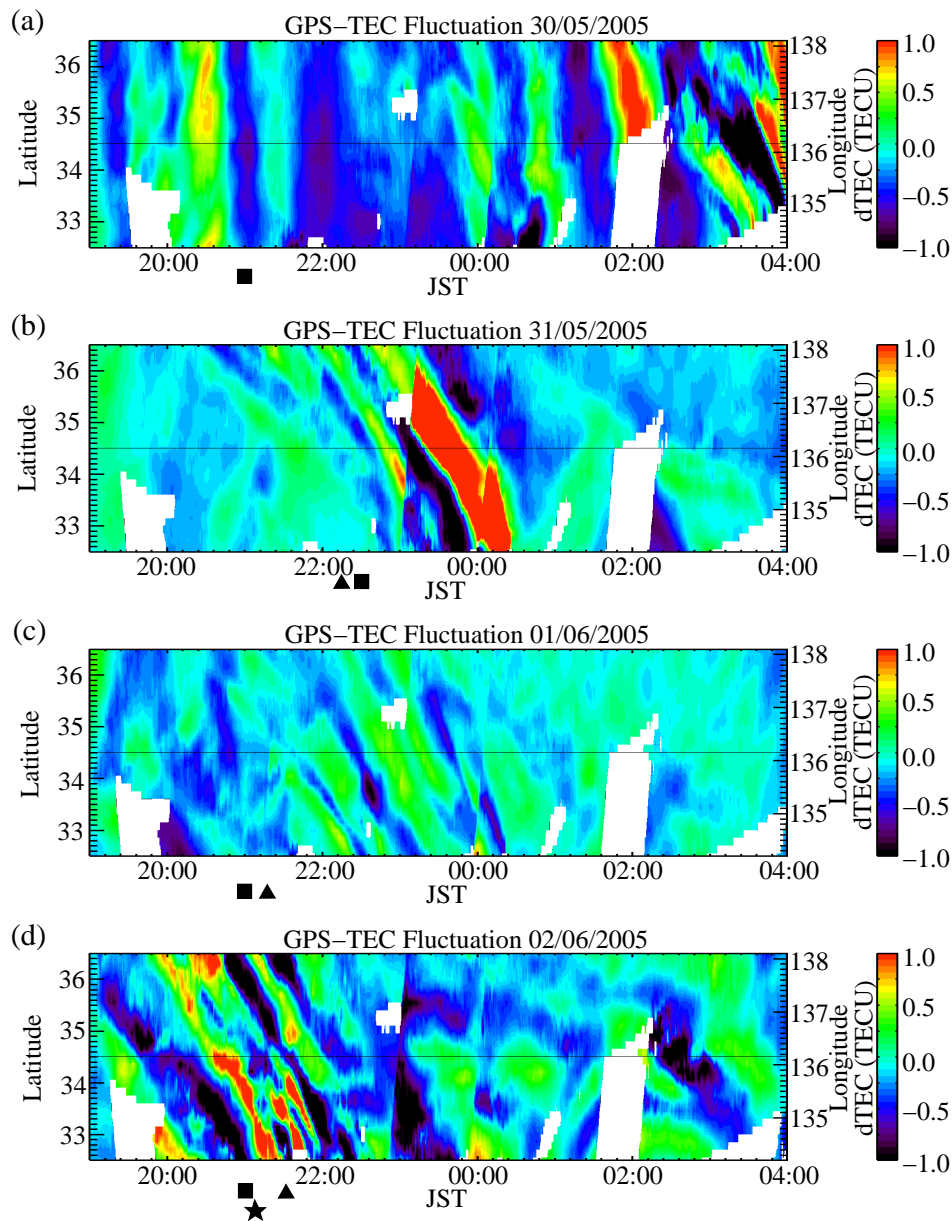
Fig. 4. TEC variation along the line from northeast to southwest indicated in Fig. 1 in keogram format. **(a–d)** correspond to four successive nights from 30 May to 2 June 2005, respectively. The Horizontal line in each plot show the point connected to the E region at an altitude of 100 km observed with the MU radar. Squares (□), a star (⋆), and triangles (△) in the figures show the time of events in Figs. 3, 5, and 6, respectively.

other examples of radar images and their relationship to the TEC variations that are field-associated. The events are selected from times designated by triangle symbols in Figs. 2 and 4. Band structures in the E region were observed when MSTIDs were active. The hypothesis of Hysell et al. (2002) that the ribbon structure might be related to MSTIDs was verified for the first time by our observations. The band structures were found at various phases of MSTIDs. But we found good overall alignment of their phase fronts. The typical distances between the E-region band structures (∼10 km) were

much smaller than the typical wavelength of the F-region MSTIDs (∼150 km), i.e., there were several bands of the E-region echoes within one wavelength of the MSTIDs.

3.3 Doppler velocity of QP Echoes and MSTIDs

Figure 7 shows the Doppler velocity of QP echoes for the three nights when QP echoes and MSTIDs were observed. The Doppler velocity of QP echoes appears to be quasi-periodically modulated. However, the period of the Doppler
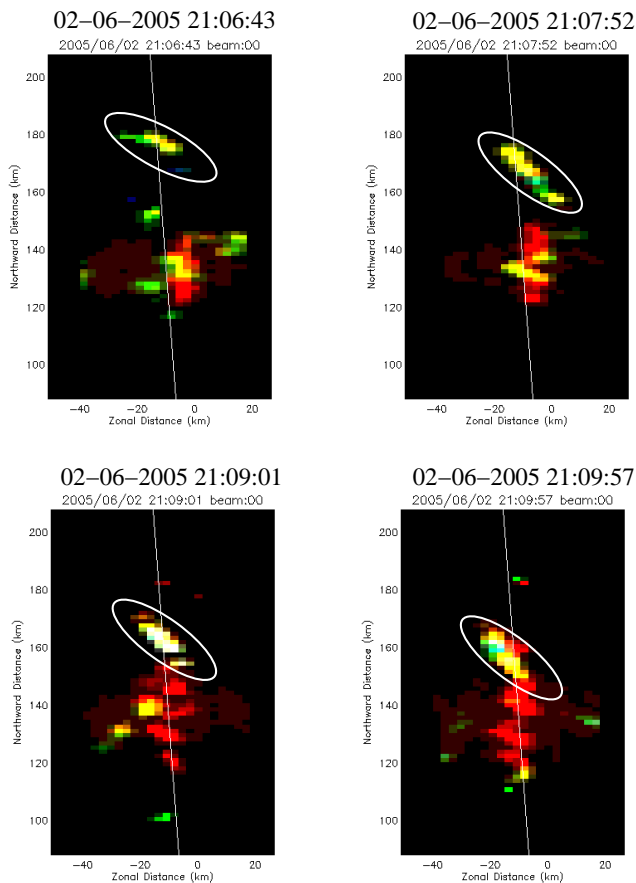
Fig. 5. Radar interferometric images of QP echoes observed from 21:06:43 to 21:09:57 JST (from top-left to bottom-right) on 2 June 2005 mapped along the geomagnetic field line on the horizontal plane at an altitude of 100 km. The time when these images were obtained is indicated by a star (⋆) in Figs. 2 and 4. The dashed lines show the center of the radar beam.

velocity variation of the QP echoes is longer than that of the echo power variation seen as QP striations. The period is rather close to that of MSTIDs. This indicates that the Doppler velocity of QP echoes could be modulated by the electric field of the MSTIDs. The maximum peak-to-peak amplitudes of Doppler velocities of QP echoes and TEC variations of MSTIDs at the field-associated F region for the three nights are summarized in Table 2. The larger the amplitude of MSTIDs was, the faster the Doppler velocity of QP echoes appeared to be. Figure 8 shows a precise comparison between the Doppler velocity of QP echoes and the TEC variation from 21:00 to 22:00 JST on 2 June 2005, when the MSTIDs were most active. When TEC variation was negative (positive), the Doppler velocity tended to be positive (negative). The agreement of phases of the TEC variation and the Doppler velocity of QP echoes was not perfect. However, their variation periods are similar to each other. It should be noted that the period of the Doppler velocity varia-

tions are clearly longer than that of the echo power variation In a precise comparison between the TEC variation and the QP echoes, we should be careful as the spatial distribution of TEC may shift depending on the assumed altitude of the F-region peak. In our analysis the altitude is assumed to be 300 km. We checked that the Ionosonde at the MU radar site showed altitudes of the F-region peak between 300 and 330 km in this period. The horizontal shift of the TEC distribution associated with the 30 km variation of ionospheric altitude is in the worst case 37 km; that is one-fourth of the observed wavelength. The slight difference between the phases of the TEC variation and the Doppler velocity variation could be due to the uncertainty of ionospheric altitudes.

4 Discussion

4.1 Coincidence of QP echoes and MSTIDs

Important finding from our experiment is that QP echoes and MSTIDs appeared and disappeared simultaneously (Table 1). The irregularities in the E region (QP echoes) and the F region (MSTIDs) were very likely closely coupled. The simultaneous appearances/disappearances of QP echoes and MSTIDs suggest that both irregularities share the same instability conditions. The period 02:30–04:30 JST on 31 May 2005 was the only exception from the other three cases, when MSTIDs were active but QP echoes were not very active. The ionosonde at the MU radar site, however, observed the strong and inhomogeneous E_s layer 02:30–04:30 JST on 31 May 2005. f_oE_s and f_bE_s over the MU radar, which, respectively, correspond to the highest and lowest plasma density in E_s layers, were 8.5 MHz (9×10^{11} m^{-3}) and 2 MHz (5×10^{10} m^{-3}). QP echoes are known to be closely related to large $f_oE_s - f_bE_s$ (Ogawa et al., 2002; Maruyama et al., 2006). In fact, we find a few faint striations of E region echoes in this time period. This fact may suggest that some unknown factors were missing at this time period and the 3-m scale irregularities were not fully developed to the level detectable by the MU radar. Summarizing the discussion, we found that for all four cases the MSTIDs in the F region were well associated with the inhomogeneous E_s layer, and three of four cases were coincided with intense QP echoes.

4.2 Coupling processes between the E- and F region

Using 630.0 nm airglow images and plasma drift velocity measurements obtained with the DMSP satellites that flew over the ionosphere, Shiokawa et al. (2003b) have shown that strong electric field is associated with MSTIDs. Since the magnetic field line is essentially equipotential, electric field perpendicular to the magnetic field line with the spatial scale of MSTIDs should be mapped down to the E region. Haldoupis et al. (2003) have proposed that the polarization electric field induced in the E region could be mapped to the F region and generate F-region irregularities. We did not
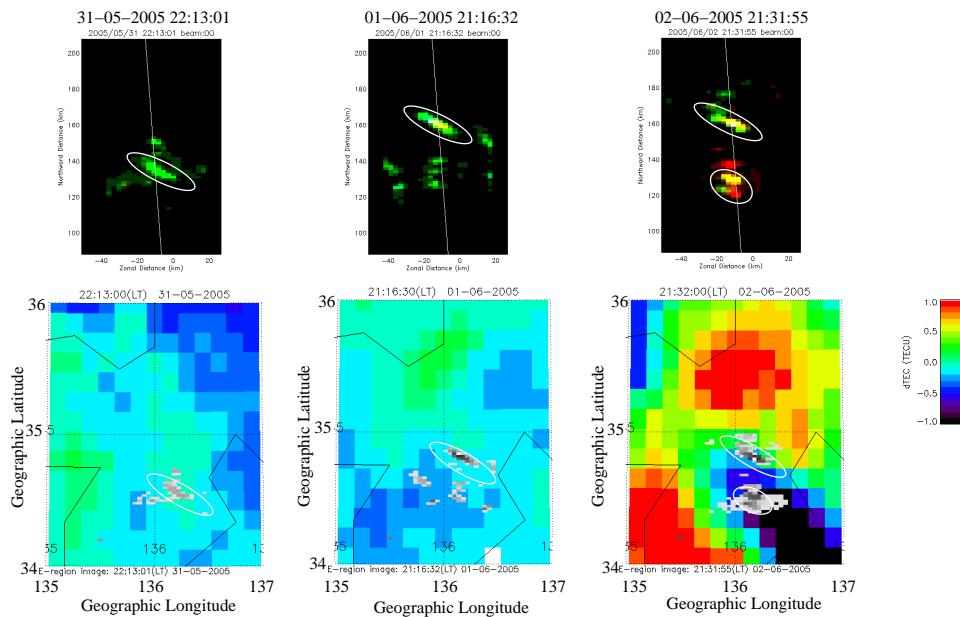
Fig. 6. Images of QP echoes mapped to 300 km altitude along the geomagnetic field lines observed at 22:13:01 JST on 31 May 2005, 21:16:32 JST on 1 June 2005, and 21:31:55 JST on 2 June 2005 (triangles (△) in Figs. 2 and 4). TEC perturbation maps closest in time to the QP echo images are also shown.

clearly observed electric field fluctuation with a scale of QP echo patches in the observations reported here. Instead, we found that the E-region Doppler velocity of the QP echoes fluctuated with the time scale of the MSTIDs. The modulation of the Doppler velocity of QP echoes should be ascribed to the electric field in the F region associated with MSTIDs.

One of the remaining problems is that of which is the source, the E- or F region. Cosgrove and Tsunoda (2002) have proposed a theory that the E_s layer at a wind shear node is in itself unstable and that the preferred propagation directions of the instability are southwestward in the Northern Hemisphere and northwestward in the Southern Hemisphere. This could be accelerated through the E-F coupled layer instability (Cosgrove and Tsunoda, 2004). In their coupling model, the wind shear in the E region is the source of instability. Kelley and Fukao (1991) proposed that gravity waves may be a seed to cause the Perkins instability. Although the growth rate of the pure Perkins instability is too small, the E-F layer coupled instability could accelerate the seed perturbation when the condition of the E_s layer for the instability is satisfied. In this case, the source of the instability is in the F region. It is difficult to determine from our observations which is the source, the E region or the F region.

Abdu et al. (2003) has shown that an upward (downward) electric field imposed on the E region could form (disrupt) the E_s layer. The electric field associated with MSTIDs are perpendicular to the wavefront (Shiokawa et al., 2003b); northeastward or southwestward. Because of inclination of the geomagnetic field (~49°), the northeastward (southwestward) electric field has upward (downward) component, un-

less the electric field has a component parallel to the magnetic field. Since QP echoes were observed at any phases of MSTIDs, it is not likely that the vertical electric field associated with MSTIDs are responsible for the E_s layer occurrences that are necessary for QP echoes.

We should note that the observed horizontal scale of QP echoes (~10 km) is much smaller than that of MSTIDs (~150 km). This is different from the postulated situation in the preceding E-F region coupling models, where both regions are perturbed at the same wave length (Haldoupis et al., 2003; Cosgrove and Tsunoda, 2004). The E_s layer is known to be very inhomogeneous when QP echoes are observed (Ogawa et al., 2002; Maruyama et al., 2006). In our experiment, for example, when well-defined QP echoes were observed on 2 June 2006, the lowest electron density of the E_s layer over the MU radar site was 6.0×10^{10} m^{-3} ($f_b E_s$=2.2 MHz) which was less than 1/20 of the highest (1.4×10^{12} m^{-3}, $f_o E_s$=10.5 MHz). As far as the perturbations in the E and F regions are in the same scale sizes, their models expect that this inhomogeneity helps to accelerate plasma instability in both regions through mapping of the electric field. When the spatial scale of the inhomogeneity of the E_s layer is much smaller than that of the F region perturbation, the effective Pedersen conductivity in the E-F region coupling process is significantly reduced, and for example, the Cosgrove and Tsunoda (2004)'s model would suffer. The inhomogeneous E_s layer would generate the polarization electric field at the scale size of its inhomogeneity. The scale of QP echoes (~10 km) is comparable to the smallest scale size (~15 km) that could be mapped to the F region
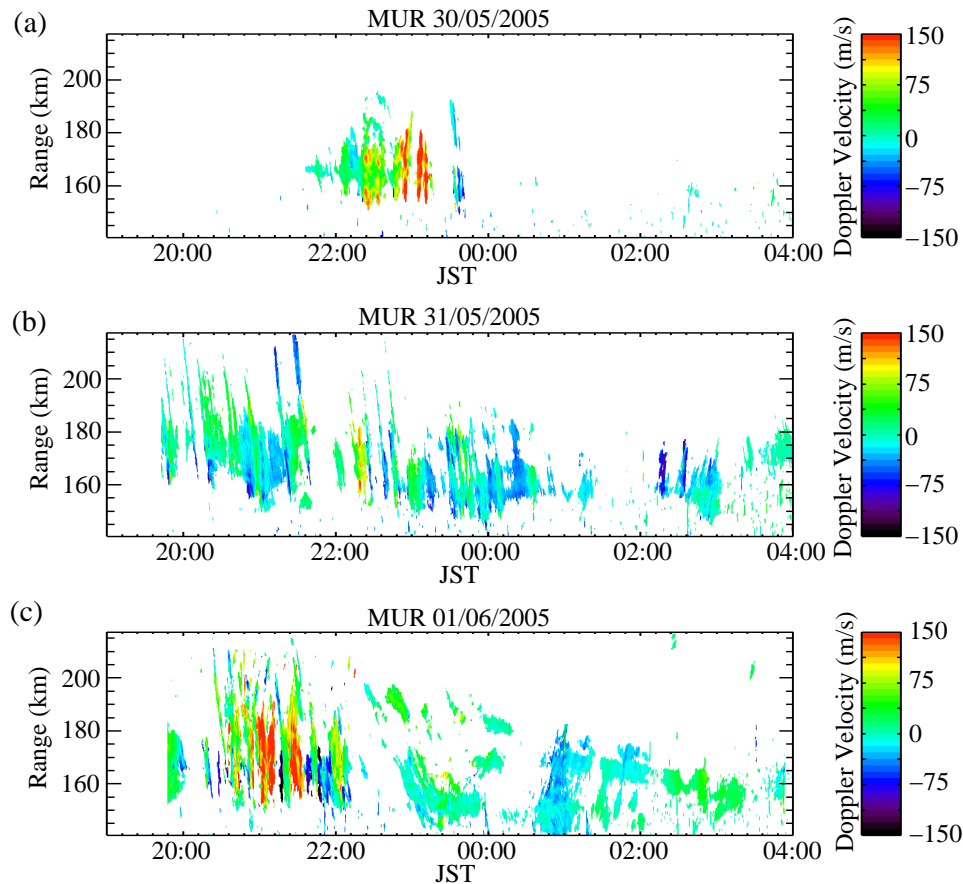
Fig. 7. Doppler velocity observed with the MU radar and presented in RTI format. **(a–c)** correspond to three successive nights from 31 May to 2 June 2005, respectively. The positive (negative) Doppler velocity refers to motion away from (toward) the radar.

given by Haldoupis et al. (2003). So it is marginal whether the polarization electric field generated in the E region can be mapped to the F region and make a structures in the F region at the scale size of the QP echoes. This point needs more investigation. In the future experiment, we should enhance spatial resolution for the F region measurement so that we could look for plasma structure as small as the QP echoes in the E region.

4.3 Implication to the seasonal variation of MSTID occurrences

MSTID activities over Japan are known to have a major peak in May–July, and a second minor peak in November–February, and to be less active in equinoxes (Shiokawa et al., 2003a). Shiokawa et al. (2003a) have attributed the double peaks in MSTID occurrence to the seasonal variation of neutral density or that of atmospheric gravity wave activity, that could seed MSTIDs. Otsuka et al. (2004) has shown that MSTIDs are simultaneously observed at the magnetic conjugate points in Japan and Australia with a good symmetry. In other words, MSTIDs exist simultaneously in both

the hemispheres propagating southwestward in the Northern Hemisphere and northwestward in the Southern Hemisphere. The E_s layer is often observed in local summer in the midlatitude ionosphere in the Asian-Oceanian sector (Taguchi and Shibata, 1961; Wu et al., 2005). From our observations of the close relationship between MSTIDs and the E_s layer, we suggest that the seasonal variations of MSTID occurrence could be attributed to E_s layer activity. That is, the E_s layer over Japan may play an important role in generating MSTIDs in the summer in Japan through the coupling process, and the E_s layer over Australia may play an important role in generating them in Japan in winter. To confirm this, observations of both MSTIDs and irregularities associated with the E_s layer at the magnetic conjugate points are necessary.

5 Conclusion

We observed MSTIDs in the F region that were connected to the E region where well-defined QP echoes were observed simultaneously. Onset and termination of well-defined QP echoes and MSTIDs were well coincided. Band
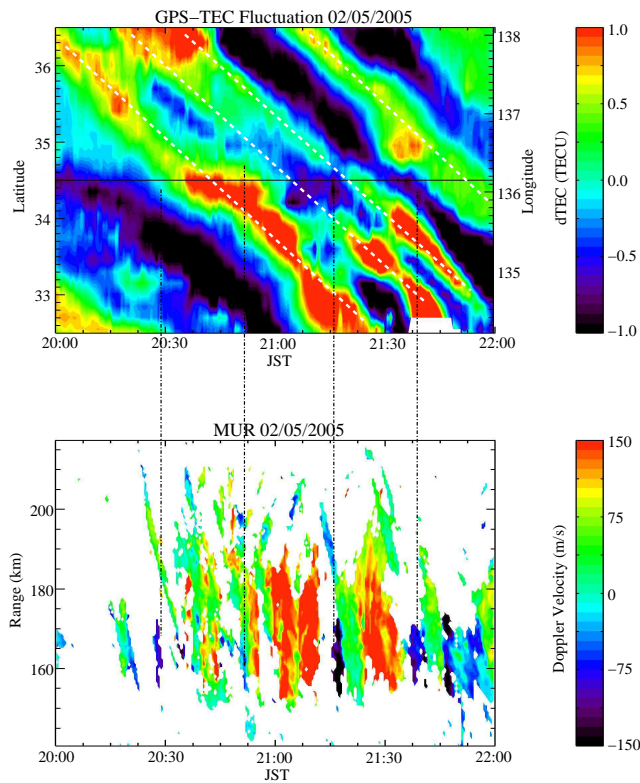
Fig. 8. Close-up of TEC-keogram and an RTI plot of QP echo powers between 21:00 and 22:00 JST on 2 June 2005.

("ribbon" (Hysell et al., 2002)) structure in QP echoes and MSTIDs were observed simultaneously. Their wavefronts were aligned in the same direction, NW–SE, and they propagated in the same direction, SW, with similar velocities. These results show that MSTIDs and the E_s layer are closely coupled in their generation processes. However, the spatial scale of QP echoes was much smaller than that of MSTIDs. This cannot simply be explained by the E-F coupled instability proposed by Cosgrove and Tsunoda (2002). From the present study, determining which is the source, the E region or the F region is difficult. Observations of both MSTIDs and irregularities associated with the E_s layer at the magnetic conjugate points are necessary to investigate whether the E_s layer may modulate ionospheric structures in the other hemisphere by electric coupling through the geomagnetic field line.

References

Abdu, M. A., MacDougall, J. W., Batista, I. S., Sobral, J. H. A., and Jayachandran, P. T.: Equatorial evening prereversal electric field enhancement and Sporadic E layer disruption: A manifestation of E and F region coupling, J. Geophys. Res., 108, 1254, doi:10.1029/2002JA009285, 2003.

Cosgrove, R. B. and Tsunoda, R. T.: A direction dependent instability of sporadic-E layers in the nighttime midlatitude ionosphere, Geophys. Res. Lett., 29, 11–1, doi:1029/2002GL014669, 2002.

Cosgrove, R. B. and Tsunoda, R. T.: Instability of the E-F coupled nighttime midlatitude ionosphere, J. Geophys. Res., 109, A04305, doi:10.1029/2003JA010243, 2004.

Fukao, S., Kelley, M. C., Shirakawa, T., Takami, T., Yamamoto, M., Tsuda, T., and Kato, S.: Turbulent upwelling of the midlatitude ionosphere 1., Observational results by the MU radar, J. Geophys. Res., 96, 3725–3746, 1991.

Garcia, F. J., Kelley, M. C., Makela, J. J., and Huang, C.-S.: Airglow observations of mesoscale low-velocity traveling ionospheric disturbances at mid-latitudes, J. Geophys. Res., 105, 18 407–18 416, 2000.

Haldoupis, C., Kelley, M. C., Hussey, G. C., and Shamilov, S.: Role of unstable sporadic-E layers in the generation of midlatitude Spread F, J. Geophys. Res., 108, SIA 11-1, doi:10.1029/2003JA009956, 2003.

Hysell, D. L., Yamamoto, M., and Fukao, S.: Imaging radar observations and theory of type I and type II quasi-periodic echoes, J. Geophys. Res., 107, SIA 7-1, doi:10:1029/2002JA009292, 2002.

Kelley, M. C. and Fukao, S.: Turbulent upwelling of the midlatitude ionosphere, 2., Theoretical framework, J. Geophys. Res., 96, 3747–3753, 1991.

Kelley, M. C., Haldoupis, C., Nicolls, M. J., Makela, J. J., Belehaki, A., Shamilov, S., and Wong, V. K.: Case studies of coupling between the E and F regions during unstable sporadic-E conditions, J. Geophys. Res., 108, SIA 12-1, doi:10.1029/2003JA009955, 2003.

Kubota, M., Shiokawa, K., Ejiri, M. K., Ogawa, T., Sakanoi, T., Fukunishi, H., Yamamoto, M., Fukao, S., Saito, A., and Miyazaki, S.: Tracking of wave- like structures in the OI 630-nm nightglow over Japan using an all- sky imagers network during FRONT campaign, Geophys. Res. Lett., 27, 4037–4040, 2000.

Maruyama, T., Saito, S., Yamamoto, M., and Fukao, S.: Simultaneous observation of sporadic E with a rapid-run ionosonde and VHF coherent backscatter radar, Ann. Geophys., 24, 153–162, 2006,

Mendillo, M., Baumgardner, Nottingham, J., Aarons, J., Reinish, B., Scali, J., and Kelley, M. C.: Investigations of thermospheric-ionospheric dynamics with 6300-Å images from the Arecibo observatory, J. Geophys. Res., 102, 7331–7343, 1997.

Ogawa T., Takahashi, O., Otsuka, Y., Nozaki, K., Yamamoto, M., and Kita, K.: Simultaneous middle and upper atmosphere radar and ionospheric sounder observations of midlatitude E region irregularities and sporadic E layer, J. Geophys. Res., 107(A10), 1275, doi:10.1029/2001JA900176, 2002.

Otsuka, Y., Shiokawa, K., Ogawa, T., and Wilkinson, P.: Geomagnetic conjugate observations of medium-scale traveling ionospheric disturbances at midlatitude using all-sky airglow imagers, Geophys. Res. Lett., 31, L15803, doi:10.1029/2004GL020262, 2004.

Perkins, F.: Spread F and ionospheric currents, J. Geophys. Res.,

78, 218–226, 1973.

Saito, A., Fukao, S., and Miyazaki, S.: High resolution mapping of TEC perturbations with the GSI GPS network over Japan, Geophys. Res. Lett., 25, 3079–3082, 1998.

Saito, A., Nishimura, M., Yamamoto, M., Fukao, S., Tsugawa, T., Otsuka, Y., Miyazaki, S., and Kelley, M. C.: Observations of traveling ionospheric disturbances and 3-m scale irregularities in the nighttime F-region ionosphere with the MU radar and a GPS network, Earth Planets and Space, 54, 31–44, 2002.

Saito, S., Yamamoto, M., Hashiguchi, H., and Maegawa, A.: Observation of three-dimensional structures of the quasi-periodic echoes associated with mid-latitude sporadic-E layers by the MU radar ultra-multi-channel system, Geophys. Res. Lett., 33, L14109, doi:10.1029/2005GL025526, 2006.

Shiokawa, K., Ihara, C., Otsuka, Y., and Ogawa, T.: Statistical study of nighttime medium-scale traveling ionospheric disturbances using midlatitude airglow images, J. Geophys. Res., 108, SIA 13-1, doi:10.1029/2002JA009491, 2003a.

Shiokawa, K., Otsuka, Y., Ihara, C., Ogawa, T., and Rich, F. J.: Ground and satellite observations of nighttime medium-scale traveling ionospheric disturbance at midlatitude, J. Geophys. Res., 108, SIA 3-1, doi:10.1029/2002JA009639, 2003b.

Taguchi, S. and Shibata, H.: World maps of f_oE_s, J. Radio Res. Lab., 8, 355–389, 1961.

Tsunoda, R. T., and Cosgrove, R. B.: Coupled electrodynamics in the nighttime midlatitude ionosphere, Geophys. Res. Lett., 28, 4171–4174, 2001.

Tsunoda, R. T., Cosgrove, R. B., and Ogawa, T.: Azimuth dependent E_s layer instability: A missing link found, J. Geophys. Res., 109, A12303, doi:10.1029/2004JA010597, 2004.

Wu, D. L., Ao, C. O., Hajj, G. A., de la Torre Juarez, M., and Mannucci, A. J.: Sporadic E morphology from GPS-CHAMP radio occultation, J. Geophys. Res., 110, A01306, doi:10.1029/2004JA010701, 2005.

Yamamoto, M., Fukao, S., Woodman, R. F., Ogawa, T., Tsuda, T., and Kato, S.: Mid-latitude E region field-aligned irregularities observed with the MU radar, J. Geophys. Res., 96, 15943–15949, 1991.

Yamamoto, M., Fukao, S., Tsunoda, R. T., Igarashi, K., and Ogawa, T.: Preliminary results from joint measurements of E-region field-aligned irregularities using the MU radar and the frequency-agile radar, J. Atmos. Terr. Phys., 59, 1655–1663, 1997.